

**COVER ARTICLE**

Laskin *et al.*  
Soft-landing of peptide ions onto self-assembled monolayer surfaces: an overview

**ARTICLE**

Hermans *et al.*  
Pronounced non-Arrhenius behaviour of hydrogen-abstractions from toluene and derivatives by phthalimide-*N*-oxyl radicals

# Soft-landing of peptide ions onto self-assembled monolayer surfaces: an overview

Julia Laskin,\* Peng Wang and Omar Hadjar

Received 17th August 2007, Accepted 23rd November 2007

First published as an Advance Article on the web 18th December 2007

DOI: 10.1039/b712710c

This review is focused on what has been learned in recent research studies concerned with fundamental aspects of soft-landing and reactive landing of peptide ions on self-assembled monolayer surfaces (SAMs). Peptide ions are particularly attractive model systems that provide important insights on the behavior of soft landed proteins, while SAMs provide a convenient and flexible platform for tailoring the interfacial properties of metals and semiconductor surfaces. Deposition of mass-selected ions on surfaces is accompanied by a number of processes including charge reduction, neutralization, covalent and non-covalent binding, and thermal desorption of ions and molecules from the substrate. Factors that affect the competition between these processes are discussed.

## Introduction

Interaction of hyperthermal (< 100 eV) beams of mass selected ions with suitable targets can be utilized for controlled modification of the physical and chemical properties of surfaces.<sup>1–3</sup> Two major physical processes dominant in this energy regime of ion–surface collisions are scattering and deposition of ions onto surfaces.<sup>4–9</sup> Soft-landing of ions on surfaces, first introduced by Cooks and co-workers,<sup>10</sup> refers to the deposition of intact projectile ions onto targets with or without the retention of the initial charge. This process has been subsequently utilized for deposition of small molecules,<sup>11–15</sup> clusters,<sup>16–22</sup>

peptides,<sup>23–26</sup> proteins,<sup>23,27,28</sup> oligonucleotides<sup>29</sup> and even viruses<sup>30</sup> onto different substrates. Deposition of low-energy ions on liquid surfaces has been used to investigate transport properties of small ions through thin and thick films.<sup>31,32</sup> Gas-phase ion chemistry combined with soft-landing provides a unique opportunity for preparation of novel synthetic materials. For example, Cooks and co-workers demonstrated chiral enrichment in the products of soft-landing of protonated serine octamers.<sup>33</sup> Castleman and co-workers used soft-landing as a tool for selective isolation of metal–carbon clusters (Met-Cars) that cannot be synthesized in the condensed phase.<sup>34</sup> Kappes and co-workers prepared novel semiconducting materials with varying electronic properties by deposition of mass-selected carbon clusters ( $C_{2n}^+$ ,  $25 \leq n < 30$ ).<sup>35</sup> Ordered nanoscale semiconducting supramolecular architectures have been prepared using soft-landing of synthetic nanographenes generated by matrix-assisted laser desorption

Fundamental Sciences Division, Pacific Northwest National Laboratory, P.O. Box 999 K8-88, Richland, WA 99352, USA.  
E-mail: Julia.Laskin@pnl.gov; Fax: (509) 376 6066;  
Tel: (509) 376 4443



Julia Laskin is a senior research scientist at the Pacific Northwest National Laboratory (PNNL). She received her MSc degree in Physics from the Leningrad

Polytechnical Institute in 1990 and her PhD in 1998 from the Hebrew University of Jerusalem. She became a permanent PNNL staff member in 2003. Her current research group utilizes ion–surface collisions for studying soft- and reactive landing of biomolecular ions on surfaces, preparing novel materials, understanding factors that determine activation and dissociation of gas-phase biomolecules and non-covalent complexes.

Peng Wang is a postdoctoral researcher at the Pacific Northwest National Laboratory (PNNL). She received her PhD from the Department of Chemistry at the University of California, Davis in 2005. Her current research conducted with Dr Julia Laskin at PNNL is mainly focused on soft landing of biomolecular ions on surfaces, among which two exciting directions are covalent immobilization of peptides on self-assembled monolayer (SAM) surfaces by reactive landing of mass selected ions and preparation of conformation-specific peptide arrays.

Omar Hadjar received his PhD in Atomic and Molecular physics from the Royal University of Groningen Netherlands in 2001. After a being a postdoc at the Center of Isotopes Research in Groningen, Netherlands, in the field of infrared spectroscopy he moved to the University of Science in Trento, Italy, working on charge transfer at hyperthermal collisions. He moved to his present position, postdoc at the Pacific Northwest National Laboratory in Richland Washington in 2005 where he is working on soft landing of biomolecular ions and mass spectrometry instrumentation.

ionization (MALDI) onto the highly ordered pyrolytic graphite (HOPG) surfaces.<sup>36</sup> Finally, we note that several studies demonstrated reactive landing (RL), in which soft-landing is followed by covalent linking of the landed species to the surface, following collisions of gas-phase ions with reactive surfaces.<sup>12,26,28,37</sup>

We recently became interested in understanding factors that affect soft-landing of peptide ions onto inert and reactive self-assembled monolayer (SAM) surfaces.<sup>8,24,25,38–41</sup> Surfaces modified with peptides are commonly used in biological and medical applications ranging from characterization of molecular recognition events at the amino acid level and identification of biologically active motifs in proteins to the development of novel biosensors and substrates for improved cell adhesion.<sup>42,43</sup> These studies commonly utilize SAMs because of their well-defined structure, controllable surface properties and biocompatibility.<sup>42</sup> In addition, controlled deposition of peptide and protein ions onto surfaces presents a new approach for obtaining molecular level understanding of interactions of biomolecules and biomolecular ions with a variety of hydrophobic and hydrophilic substrates. In our studies we explored the effect of the primary structure of the ion, its kinetic energy and initial charge state, physical and chemical properties of SAM surfaces on the efficiency of soft-landing and reactive landing. In this article we present a summary of our current understanding of the fundamentals of these processes.

## Instrumentation

### Ion deposition

Instrumentation developed for studying interactions of polyatomic hyperthermal ions with surfaces has been extensively reviewed<sup>1,8,9</sup> and will not be discussed in this paper. Soft-landing experiments conducted in our laboratory utilized a newly constructed ion deposition instrument shown in Fig. 1<sup>44</sup> and a custom built 6T Fourier transform ion cyclotron resonance (FT-ICR) instrument specially configured for studying ion–surface interactions<sup>24,45</sup> (Fig. 2). The design of an ion source is similar for both instruments. Ions are produced in an electrospray ionization (ESI) source and introduced into the vacuum system using an electrodynamic ion funnel. Ions exiting the ion funnel undergo collisional relaxation in a collisional quadrupole (CQ) followed by mass selection using a quadrupole mass filter (resolving quadrupole, RQ). Mass-selected ions are transmitted through a series of Einzel lenses that enable precise positioning and shaping of the ion beam. An electrostatic quadrupole bender located after the second Einzel lens turns the ion beam by 90° to avoid contamination of the surface by neutrals. The ion beam is further focused using two additional Einzel lenses, decelerated between two meshes and allowed to collide with the surface. Ion collision energy is determined by the difference between the dc offset of the CQ and the potential applied to the surface. Lowering the voltage applied to the surface increases the collision energy for positive ions. Visualization of the ion beam prior to the deposition has been implemented in the instrument shown in Fig. 1. It enables precise control of the

size and position of the ion beam for deposition of a single or multiple spots on the surface. A similar approach is used for soft-landing of mass-selected ions using the FT-ICR SIMS apparatus shown in Fig. 2. In this system the surface is positioned at the rear trapping plate of the ICR cell that is located inside the strong magnetic field. Detailed description of the ion deposition experiment in the FT-ICR instrument was presented elsewhere.<sup>24,38</sup>

### Amount of deposited material

The amount of material deposited by soft-landing is in general difficult to quantify. The upper limit estimate can be obtained from the measurement of the ion current delivered to the substrate. Typical ion currents of mass selected ions that can be delivered to the surface range from several picoamperes to several nanoamperes corresponding to the deposition of 0.1–100 ng of material in 1 h for molecules with molecular weight of 1000 amu. However, because of the scattering of ions off the surface that occurs on a very short time scale and slow desorption of ions or molecules from the surface, the actual amount of material retained on the target may be significantly smaller. The scattering efficiency strongly depends on the properties of the SAM layer and can reach 50–60% for the fluorinated SAM (FSAM) surfaces.<sup>7,46</sup> Wysocki and co-workers found that for small open-shell projectile ions colliding with different SAMs the decrease in the total signal of scattered ions was accompanied by an increase in the ion current measured on the surface.<sup>47,48</sup> They concluded that SAMs which efficiently block the electron transfer give the lowest measured current on the surface and suggested that the ion current measured on the surface is indicative of the neutralization efficiency of the projectile ions. In our experience such behavior is not observed during collisions of peptide ions with different SAM surfaces (*i.e.* the measured current does not depend on the properties of the SAM surface). This could be attributed to the differences in the neutralization mechanisms between closed-shell peptide ions and open-shell radical cations studied by the Wysocki group. It should be noted that neutralization is not required for the observation of the ion current on the surface because each ion approaching the target attracts an electron. SAMs can be viewed as thin insulating layers on metal substrates characterized by fairly high capacitance. Ions striking the SAM surface attract electrons to the opposite side of the capacitor. Electron transport through well-organized SAMs of alkylthiols and fluorinated alkylthiols is a fairly slow process. The electron transfer rate of  $10^{-19}$  C s<sup>-1</sup> is estimated based on the values of capacitance (*ca.* 1  $\mu$ F cm<sup>-2</sup>) and resistance (*ca.* 10<sup>6</sup>  $\Omega$  cm<sup>2</sup>) reported in the literature.<sup>49</sup>

From the above discussion it follows that for collisions of even-electron peptide ions with SAM surfaces measurement of the ion current on the surface provides a reasonable estimate for the amount of ions delivered to the surface. The amount of retained material depends on the properties of the projectile ion and the surface. Volny *et al.* used surface-compatible solution assay methods to determine the activity of soft-landed enzymes.<sup>28</sup> They concluded that more than 80% of enzyme molecules soft-landed onto plasma-treated silver surfaces

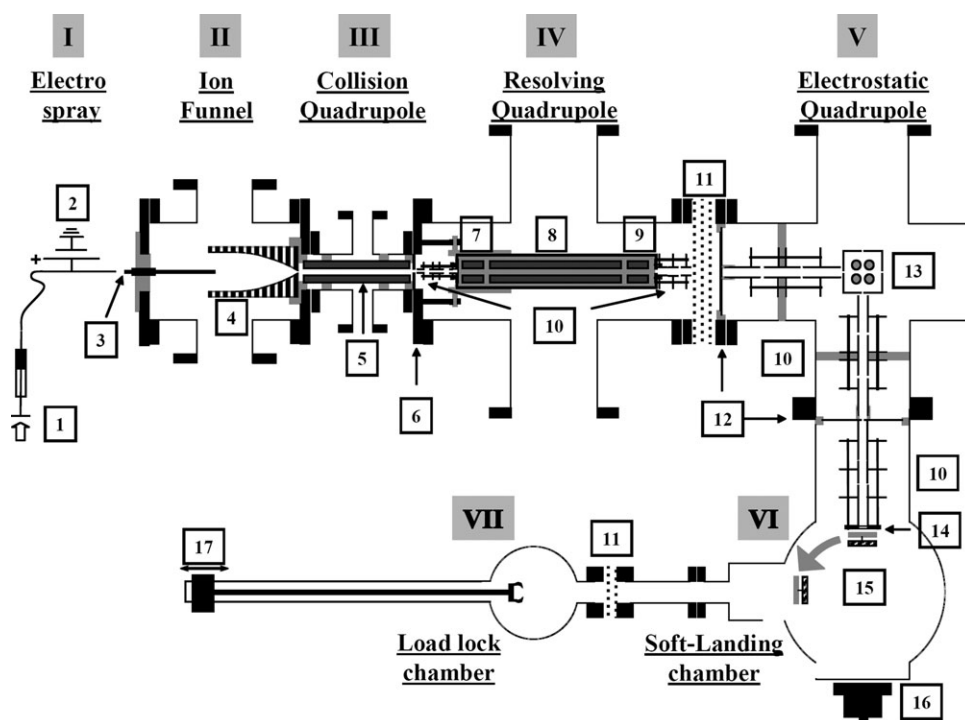


**Fig. 1** Schematic view of the ion soft landing instrument: I – electrospray source (760 Torr). II – High-transmission ion funnel ( $2 \times 10^{-1}$ Torr). III – Ion thermalization and focusing stage ( $10^{-2}$ Torr). IV –  $m/z$  ion selection stage ( $4 \times 10^{-5}$ Torr). V –  $90^\circ$  ion bending stage ( $10^{-7}$ Torr). VI – Ultra high vacuum (UHV) chamber for ion soft-landing ( $2 \times 10^{-9}$  Torr). VII – Surface introduction stage (from 760 to  $2 \times 10^{-8}$  Torr). (1) Syringe pump, (2) electrospray tip, (3) heated capillary, (4) electro-dynamic ion funnel, (5) collisional quadrupole (CQ), (6) 1 mm conductance limit, (7) pre-filter, (8) resolving quadrupole (RQ), (9) post filter, (10) Einzel lenses, (11) gate valve, (12) 2 mm conductance limit, (13) electrostatic quadrupole (bender), (14) deceleration area, (15) surface and phosphorus screen detector, (16) CCD camera, (17) magnetic translator. Reprinted with permission from Hadjar *et al.*, *Anal. Chem.*, 2007, **79**, 6566. Copyright 2007, American Chemical Society.

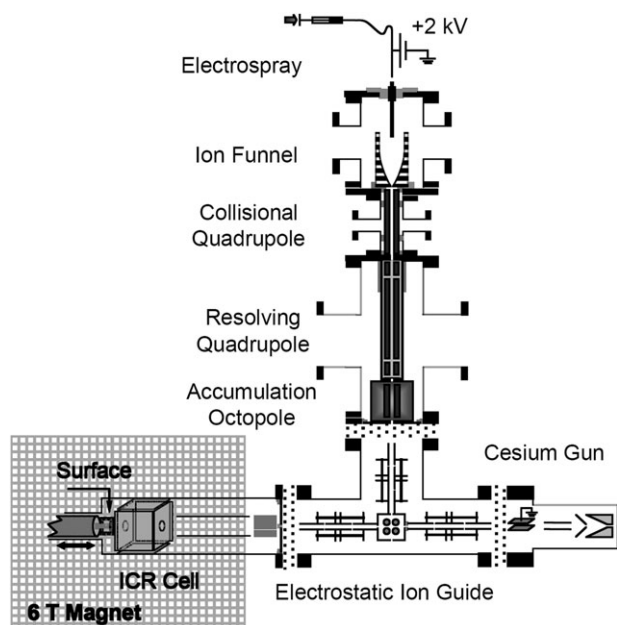


**Fig. 2** Schematic drawing of the Fourier transform ion cyclotron resonance (FT-ICR) instrument showing the electrospray interface used to generate the beam of mass-selected peptide ions and the in-line cesium gun used for *in situ* SIMS analysis of the surface. Reprinted with permission from Hadjar *et al.*, *J. Phys. Chem. C*, 2007, **111**, 18220. Copyright 2007, American Chemical Society.

retained their biological activity. Because some of the soft-landed molecules may become inactive this value presents the lower-limit estimate for the soft-landing efficiency for these systems.

We have conducted an experiment in which  $2 \times 10^{13}$   $[M + H]^+$  ions (260 pA for 3.5 h) or  $[M - H]^-$  ions (31 pA for 29 h) of KAAAA peptide were deposited onto the FSAM surface. Samples were subsequently sonicated in 1.2 mL of methanol and analyzed using electrospray ionization. Signal intensities of  $[M + H]^+$  ions obtained from the extracts were compared to the signals obtained for KAAAA solutions of known concentration. Soft-landing efficiency of  $20 \pm 3\%$  for both positive and negative ions was determined from this experiment. This value represents the lower estimate because it does not take into account slow desorption of ions and molecules from the surface following soft-landing. In addition, we noted that the loss of peptide molecules from SAM surfaces is substantially slower for larger peptides than for KAAAA suggesting that higher soft-landing efficiency would be obtained for larger projectiles.

While the soft-landing efficiency is lower than 100% it is convenient to report the amount of deposited material in terms of the ion exposure. The surface coverage reported in most studies corresponds to the number of ions delivered to the surface that is derived from the measured ion current. Clearly, these values represent the upper-limit estimate for the amount of material retained on the surface.

## Surface characterization

Physical and chemical characterization of surfaces following soft-landing is essential for understanding the underlying phenomena. The major challenge associated with surface characterization is a very small amount of material deposited on the substrate. Several surface characterization techniques have been utilized by different groups including laser desorption ionization,<sup>12,23,27,30</sup> low-energy chemical sputtering,<sup>10–12</sup> secondary ion mass spectrometry (SIMS),<sup>12,24,25,38–41</sup> surface-enhanced Raman spectroscopy (SERS),<sup>13</sup> X-ray photoelectron spectroscopy (XPS),<sup>28</sup> microscopy,<sup>16,18,34,35</sup> infrared reflection absorption spectroscopy (IRRAS),<sup>19,39–41</sup> temperature-programmed desorption (TPD)<sup>19,31,32,35</sup> and a variety of biological assays.<sup>23,27,28</sup> Studies performed in our laboratory utilize SIMS and IRRAS as complementary techniques for the analysis of soft-landing targets.

*In situ* analysis of surfaces following soft-landing is performed by combining 8 keV Cs<sup>+</sup> secondary ion mass spectrometry with FT-ICR detection of the sputtered ions (FT-ICR-SIMS).<sup>24,39</sup> SIMS experiments utilize an in-line 8 keV Cs<sup>+</sup> ion gun (Fig. 2) that allows us to interrogate the surface both during the ion deposition and after the deposition is terminated. Secondary ions produced by the 8 keV Cs<sup>+</sup> ion bombardment of the surface are trapped in the ICR cell by raising the potentials on the trapping plates 10–20 V above the cell offset and analyzed using standard procedures. *Ex situ* analysis of surfaces prepared using the ion deposition instrument (Fig. 1) is performed using time-of-flight secondary ion mass spectrometry (TOF-SIMS) and infrared reflection-absorption spectroscopy (IRRAS).

SIMS is a very sensitive technique that allows us to detect the presence of the soft-landed material even at very low coverage. We estimate that TOF-SIMS can be used to reliably detect soft-landed peptides at least at 0.05% monolayer coverage while FT-ICR SIMS experiments are sensitive to *ca.* 0.5% monolayer. At low ion dose the SIMS signal shows an almost linear increase with concentration of deposited species.<sup>24,44</sup> However, at surface coverage above 25% the signal shows a significant deviation from linearity<sup>24,44</sup> that could be attributed either to saturation of surface coverage resulting from Coulomb repulsion between ions on the surface<sup>24</sup> or to matrix effects in SIMS that have been extensively discussed in the literature.<sup>50–52</sup>

Signal suppression during the SIMS analysis of soft-landed peptide ions has been systematically studied using the HSAM and COOH-SAM as soft-landing targets.<sup>44</sup> We found that SIMS signals obtained following soft-landing of a variety of peptide ions on different SAM surfaces show a rapid decrease to zero when the amount of deposited peptide molecules on the surface exceeds 75% of a monolayer.<sup>44</sup> Furthermore we observed that high-dose deposition of peptides on surfaces results in strong suppression of all sputtered ions including those characteristic of the SAM substrate suggesting that peptide layer is a poor matrix for the formation of secondary ions.<sup>44</sup> It follows that while SIMS is a very sensitive technique for detection of soft-landed species, it can be used in a semi-quantitative way only at low surface coverage.

In contrast, the much less sensitive IRRAS technique is more quantitative because it does not suffer from surface coverage artifacts. We demonstrated that the IRRAS signal scales with the concentration of the soft-landed molecules and is capable of detecting peptide signal following deposition of more than 10% of a monolayer on a 10 mm diameter spot.<sup>40,44</sup> Our preliminary experiments indicate that IRRAS can be used to examine the secondary structure of soft-landed peptides. It should be noted that signal intensity in IRRAS experiments is determined by surface selection rules—only those vibrational modes which give rise to an oscillating dipole perpendicular to the surface contribute to the absorption. It follows that while the IRRAS signal is proportional to the concentration of deposited species it depends on the orientation of molecules on the surface and therefore caution must be taken when using IRRAS for quantitation of the amount of soft-landed molecules.

## Charge retention, charge reduction and neutralization

Charge retention by ions soft-landed onto SAM surfaces is one of the most fascinating findings reported by Cooks and co-workers in 1997.<sup>10</sup> They demonstrated that intact polyatomic ions were trapped in the FSAM for many days and could be released from the matrix by low-energy chemical sputtering or thermal desorption.<sup>10</sup> It has been suggested that the ion is well protected by the matrix and is released when the FSAM begins to break up at elevated temperatures. Partial charge retention was also observed for multiply-protonated lysozyme soft-landed onto the FSAM surface.<sup>23</sup> Charging of SAM surfaces resulting from ion deposition presents a potential concern for studying the soft-landing phenomena. If most of the ions retained their charge a significant potential could build up on the insulating surface. The potential,  $\Delta V$ , can be readily estimated using the following equation:

$$\Delta V = \frac{ZeN_{\text{ions}}d}{A\epsilon\epsilon_0} \quad (1)$$

where  $Z$  is the charge state of the ion,  $e$  is the elementary charge,  $N_{\text{ions}}$  is the number of ions on the surface,  $d$  is the thickness of the film,  $A$  is the area exposed to the ion beam,  $\epsilon_0$  is the vacuum permittivity, and  $\epsilon$  is the permittivity of the SAM. Using the dielectric constant of the SAM of 2.3 and the film thickness of 1 nm, the maximum potential of 0.9 V could be developed following 1 h exposure of the 5 mm diameter surface to 100 pA of singly charged ions ( $2.2 \times 10^{12}$  ions) assuming that all ions were trapped and remained charged following the deposition. The Coulomb force applied to the ion at a distance  $D$  from the charged thin film of radius  $R$  is given by eqn (2):

$$F = \frac{Z^2}{2\epsilon_0} \frac{N_{\text{ions}}}{A} \left( -\frac{D}{\sqrt{R^2 + D^2}} + \frac{D+d}{\sqrt{R^2 + (D+d)^2}} \right) \quad (2)$$

and the corresponding potential is given by eqn (3):

$$V = \frac{Z^2}{2\epsilon_0} \frac{N_{\text{ions}}}{A} (d + \sqrt{R^2 + D^2} - \sqrt{R^2 + (D+d)^2}) \quad (3)$$

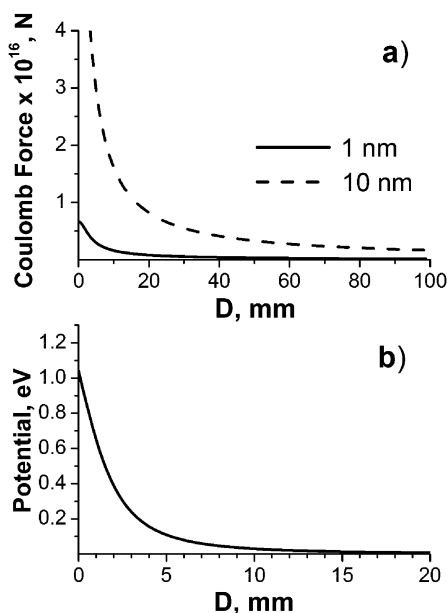


**Fig. 3** The dependence of the (a) Coulomb force and (b) the potential on the distance from the charged SAM surface for the interaction of a point charge with  $2.2 \times 10^{12}$  singly charged ions accumulated on the thin film of 5 mm diameter and 1 nm thickness. The force is shown for the film thickness of 1 and 10 nm.

Fig. 3 shows the dependence of the Coulomb force and the potential on the distance from the charged SAM surface for  $2.2 \times 10^{12}$  singly charged ions (*ca.* 25% of a monolayer) accumulated on the thin film (5 mm diameter, 1 nm thickness). Under these conditions the maximum increase in the potential is close to 1 V. In practice, this potential is substantially smaller because scattering, desorption, and partial neutralization of ions reduces the number of charged species retained on the surface. It is clear that charging phenomena may become important for relatively thick insulating films, tightly focused ion beams and long exposure times provided that the substrate retains most of the deposited charge.

Systematic studies of the soft-landing of peptide ions on surfaces demonstrated that when the FSAM surface is used as a target a substantial number of ions retain at least one proton.<sup>24,25,38</sup> These studies utilized *in situ* 2 keV Cs<sup>+</sup> FT-ICR SIMS and *ex situ* TOF-SIMS for surface characterization. We found that SIMS spectra obtained following soft-landing of multiply protonated peptides are commonly dominated by the singly protonated,  $[M + H]^+$ , species. Similar features are usually observed following the deposition of different charge states of the same peptide on the surface. However, the relative abundance of different peptide-related peaks in FT-ICR SIMS spectra depends on the initial charge of the precursor ion.<sup>38</sup> Fig. 4 compares FT-ICR spectra obtained following soft-landing of *ca.* 5% of a monolayer of singly, doubly and triply protonated substance P on the FSAM surface. It is clear that the abundance of the  $[M + 2H]^{2+}$  peak (not observed for the singly protonated precursor) and the fragmentation efficiency in SIMS spectra increases with increase in the charge state of the precursor ion. We suggested that the observed increase in the  $[M + 2H]^{2+}/[M + H]^+$  ratio with increase in the charge state of the

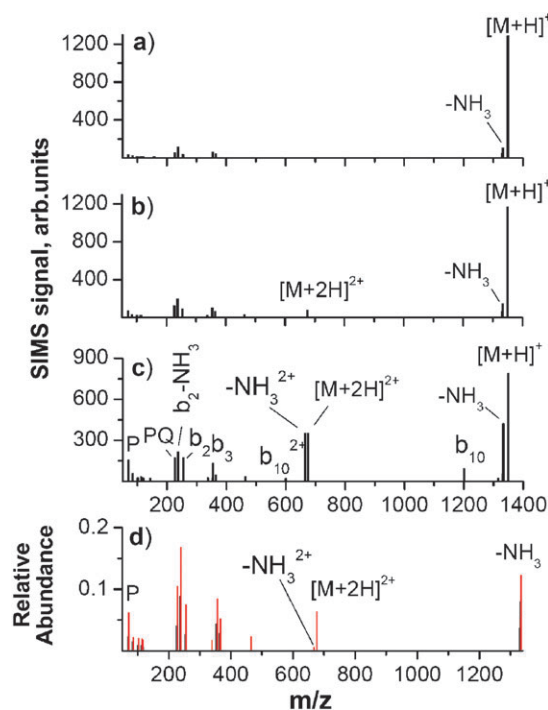


**Fig. 4** 2 keV Cs<sup>+</sup> FT-ICR-SIMS spectra of an FSAM surface following soft-landing of different charge states on Substance P ( $6.5 \times 10^{10}$  ions): (a)  $[M + H]^+$ , (b)  $[M + 2H]^{2+}$ ; (c)  $[M + 3H]^{3+}$ . Panel (d) shows a comparison of spectra shown in panels (a) and (b). All spectra are normalized to the abundance of the  $[M + H]^+$  ion. Reprinted from *Int. J. Mass. Spectrom.*, **265**, Laskin *et al.*, Charge retention by peptide ions soft-landed onto self-assembled monolayer surfaces, 237–243. Copyright 2007, with permission from Elsevier.

precursor ion could not be attributed to re-ionization of neutralized species deposited onto the FSAM surface but is indicative of charge retention by soft-landed ions. In contrast, substantially lower  $[M + 2H]^{2+}/[M + H]^+$  ratios were obtained from the TOF-SIMS analysis following soft-landing of a variety of ions onto different SAM surfaces. Because surfaces are exposed to laboratory air prior to the TOF-SIMS characterization we concluded that such exposure results in complete charge reduction of doubly protonated ions with possible retention of a fraction of  $[M + H]^+$  species. Comparison between TOF-SIMS spectra obtained following soft-landing on different SAM surfaces suggested that the neutralization efficiency increases in the order FSAM < HSAM < COOH-SAM.

It has been demonstrated that FT-ICR SIMS experiments can be used to study the decay of the SIMS signal as a function of time under ultrahigh vacuum and atmospheric pressure conditions.<sup>25</sup> Our first experiments examined the loss of the secondary ion signal following soft-landing of doubly protonated substance P (SP) onto the FSAM surface. Very different behavior in the time dependence of the SIMS signal (Fig. 5) was observed in vacuum and in air. Fast loss of the 85% of the secondary ion signal with the lifetime of 10.5 min was observed upon exposure of the surface to laboratory air followed by a slow decay of the remaining signal with lifetime of 77 min. In contrast, only the slow decay process affecting 40% of the SIMS signal was observed when the surface remained in the

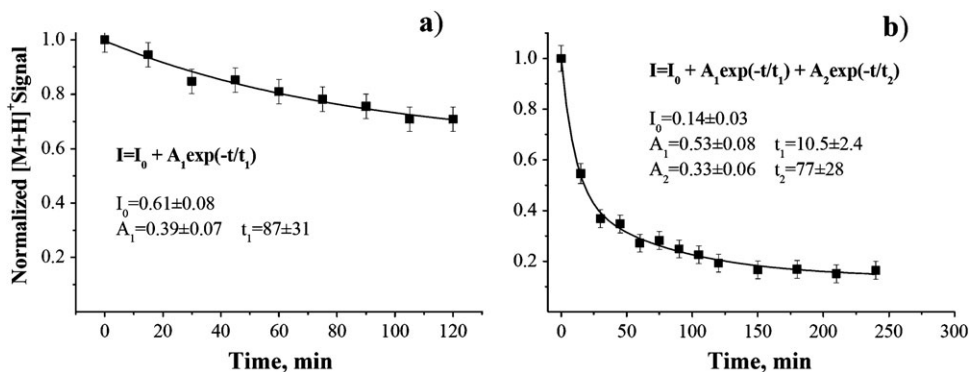


**Fig. 5** Loss of total peptide signal of Substance P soft landed on an FSAM surface as a function of time (a) under vacuum ( $2.0 \times 10^9$  Torr) and (b) under atmospheric conditions ( $7.6 \times 10^2$  Torr). Reprinted with permission from Alvarez *et al.*, *J. Phys. Chem. A*, 2006, **110**, 1678. Copyright 2006, American Chemical Society.

UHV. Because the lifetime of the slow decay component was the same in vacuum and in air we attributed the slow decay component to the same ion loss mechanism that involves desorption of ions from the surface at room temperature. Neutralization of soft landed ions upon exposure to laboratory air or fast desorption of loosely-bound species are most likely responsible for the fast component of the kinetic curve shown in Fig. 5b.

Recently we conducted a first detailed study of the kinetics of desorption and charge reduction following soft-landing of

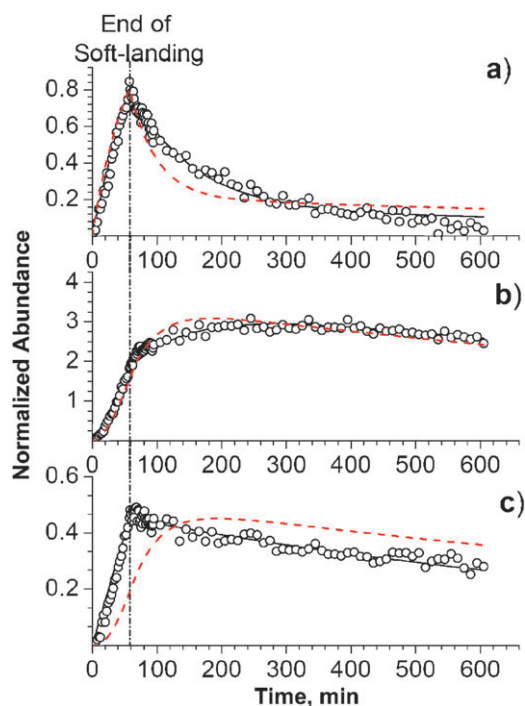


**Fig. 6** Kinetic plots obtained for the (a)  $[\text{GS} + 2\text{H}]^{2+}$  ion, (b)  $[\text{GS} + \text{H}]^+$  ion, and (c) neutral GS molecules on the surface represented by the PVO fragment ion (points) and the results of the kinetic modeling with (solid lines) and without (red dashed lines) taking into account the instantaneous charge loss by ions upon collision. Reprinted with permission from Hadjar *et al.*, *J. Phys. Chem. C*, 2007, **111**, 18220. Copyright 2007, American Chemical Society.

doubly protonated Gramicidin S (GS) onto the FSAM surface.<sup>39</sup> This study utilized an in-line 8 keV  $\text{Cs}^+$  ion gun (Fig. 2) that allowed us to interrogate the surface both during the ion deposition and after the deposition was finished. We followed the evolution of the SIMS spectrum as a function of time during 58 min of soft-landing deposition of the doubly protonated GS and for 10 h after the ion beam was switched off. The surprising discovery reported in that study was that various peptide-related peaks in FT-ICR SIMS spectra followed very different kinetics. This allowed us to obtain unique kinetics signatures for doubly protonated, singly protonated and neutral peptides retained on the surface. The corresponding kinetic plots are shown in Fig. 6. Our experimental results can be summarized as follows. We observed that the  $[\text{GS} + 2\text{H}]^{2+}$  ion deposited on the surface shows an almost linear increase during the soft-landing followed by a relatively fast depletion after ion deposition is finished. In contrast, the  $[\text{GS} + \text{H}]^+$  ion formed on the surface by partial proton loss from the soft-landed  $[\text{GS} + 2\text{H}]^{2+}$  ion, continues to increase for 2–3 h following ion deposition. Finally, we found that a majority of peptide fragments in FT-ICR SIMS spectra follow a linear increase during ion deposition and an almost linear decrease after the deposition and suggested that these fragment ions originate from neutral GS molecules on the surface.

Our results could be rationalized using a relatively simple kinetic model that incorporates charge reduction and thermal desorption of ions and neutral GS molecules from the surface. Modeling results are shown as solid lines in Fig. 6. The kinetic modeling also demonstrated the importance of the instantaneous loss of one or two protons by a fraction of ions colliding with the FSAM surface. The best fit obtained without taking into account fast proton loss is shown as dashed lines in Fig. 6. This fast charge reduction produces a mixture of different charge states of the soft-landed molecule on the surface. The resulting species undergo slow charge reduction and thermal desorption with typical rate constants ranging from  $< 10^{-5}$  to  $10^{-2} \text{ min}^{-1}$ . We found that the decay of the  $[\text{GS} + 2\text{H}]^{2+}$  signal is mainly attributed to charge reduction ( $k = 10^{-2} \text{ min}^{-1}$ ) and formation of  $[\text{GS} + \text{H}]^+$  on the surface with negligible contribution from thermal desorption ( $k < 10^{-4} \text{ min}^{-1}$ ). In contrast, the singly protonated species mainly decays by thermal desorption ( $k = 6 \times 10^{-4} \text{ min}^{-1}$ ), while

the proton loss from the  $[\text{GS} + \text{H}]^+$  ions is very slow ( $k = 1 \times 10^{-5} \text{ min}^{-1}$ ). Finally, the neutral GS molecules are formed primarily by fast neutralization of projectile ions upon collision with the surface and are slowly depopulated by desorption ( $k = 1 \times 10^{-3} \text{ min}^{-1}$ ). This technique can be utilized to obtain molecular level understanding of interactions of a variety of ions in different charge states with hydrophobic and hydrophilic mimics of biological substrates. Studies focused on deposition of different charge states of model peptides onto FSAM, HSAM and COOH-SAM surfaces are currently underway in our laboratory.

## Covalent immobilization of peptides using reactive landing

Covalent linking of molecules to substrates using soft-landing is a promising method for highly selective surface modification using hyperthermal beams of mass-selected ions. Mass spectrometry enables easy preparation of an ion of interest for subsequent deposition on a target. It effectively eliminates any separation or purification stage prior to surface modification and requires significantly smaller amounts of material than any approaches based on solution-phase reactions. Surface modification using reactive landing of low-energy ( $< 100 \text{ eV}$ ) ions has been reported by several groups. Examples include formation of silicon nitride by collisions of low-energy  $\text{N}^+$  and  $\text{N}_2^+$  ions with a Si(100) surface,<sup>53</sup> formation of Si–O bond between the OH-terminated SAM (HO-SAM) surface and a variety of  $\text{SiX}^+$  ions,<sup>54–56</sup> esterification and ether formation on the HO-SAM surface following collisions with  $\text{C}_6\text{H}_5\text{CO}^+$  and  $\text{C}_6\text{H}_5\text{CH}_2^+$  ions, respectively,<sup>57</sup> chemical modification of FSAM<sup>58–61</sup> and polystyrene<sup>62</sup> surfaces, growth and modification of thin films,<sup>2,63–65</sup> and covalent immobilization of small molecules and proteins on plasma-treated metal surfaces.<sup>26,28</sup>

Peptide-modified surfaces are commonly used in biological and medical applications ranging from characterization of molecular recognition events at the amino acid level and identification of biologically active motifs in proteins to the development of novel biosensors and substrates for improved cell adhesion.<sup>43,66</sup> Many of these applications require strong covalent binding of biological molecules to surfaces. Existing techniques for linking peptides to SAMs are based on solution-phase synthetic strategies and require relatively large quantities of purified material.<sup>66</sup> Reactive landing of peptide ions on SAM surfaces provides obvious advantages of highly specific preparation of the reactant, eliminating the effect of solvent and sample contamination on the quality of the film, shaping and precise positioning of the ion beam on the surface necessary for selective modification of specific areas on the substrate. However, it is not clear whether the reactivity between peptide molecules and SAM surfaces observed in solution can be achieved using ion–surface collisions. Understanding factors that determine the efficiency of covalent immobilization of peptides on surfaces using reactive landing is important for practical applications.

Reactive landing of RGD-containing peptide ions onto the self-assembled monolayer of N-hydroxysuccinimidyl ester terminated alkylthiol on gold (NHS-SAM) surface was studied using TOF-SIMS and IRRAS.<sup>40,41</sup> The RGD (arginine–

glycine–aspartate) motif is found in many adhesive proteins present in extracellular matrices and in the blood as their cell recognition site.<sup>67</sup> It is the shortest sequence in this class of proteins that is recognized by some integrins during cell adhesion. It has been demonstrated that RGD-containing peptides promote cell adhesion when immobilized on surfaces, and inhibit it when presented to cells in solution.<sup>68</sup> It follows that covalent linking of RGD peptides to substrates is essential for strong cell adhesion.<sup>69</sup> SAMs terminated with active esters (e.g. N-hydroxysuccinimidyl ester, NHS) are commonly used for covalent binding of peptides and proteins to substrates *via* the formation of an amide bond between the acid of the substrate and the available primary amino group of the biomolecule.<sup>70,71</sup> Optimum coupling of RGD-containing peptides to NHS-SAM surfaces in solution occurs at pH 8–9 and is complete in several hours.<sup>69</sup> It is remarkable that reactive landing of doubly protonated ions of a cyclic c-(RGDfK-) peptide on the NHS-SAM for four hours resulted in similar local surface coverage of more than 60% of a monolayer to the coverage obtained following 2 h solution-phase reaction,<sup>40</sup> while the estimated amount of material used for solution-phase surface modification was *ca.* 50 times larger than for the soft-landing experiment.

Peptides can be covalently linked to NHS-SAM surfaces *via* the N-terminal  $\alpha$ -amino group or the  $\epsilon$ -amino group of the lysine side chain. Soft-landing experiments performed for linear and cyclic peptides with and without the lysine residue demonstrated that the presence of the lysine residue significantly enhances the reaction efficiency, while the contribution of the N-terminal group to the observed reactivity is almost negligible. Fig. 7 shows the results of the TOF-SIMS and IRRAS characterization of NHS-SAM surfaces following deposition of mass-selected peptide ions (red) and after thorough rinsing of the modified surfaces in methanol (blue).<sup>41</sup> TOF-SIMS spectra contain abundant  $[\text{M} + \text{H}]^+$  ions that are readily removed by rinsing. These species are attributed to loosely bound peptides on the surface. In contrast, a number of features in the spectra are not affected by rinsing. These include the characteristic doublet of the protonated covalent adduct (CA) shown in Fig. 7, *i.e.* the peak observed at the combined molecular weight of the protonated peptide and the thiol (315.2) without the NHS endgroup (115.1) and its analog that has an additional double bond. In addition, CA cationized on gold and a series of fragment ions are commonly observed in TOF-SIMS spectra.<sup>40</sup> The fragmentation pattern produced by high-energy bombardment of the surface provides strong support for covalent binding of peptides to the NHS-SAM surface through the lysine side chain.<sup>40</sup>

IRRAS spectra display amide I and amide II bands at 1675 and 1535  $\text{cm}^{-1}$ , respectively. These features originate from peptide bonds of both loosely bound and covalently linked molecules and from the newly formed amide bond between the peptide and the SAM. Rinsing of the surface removes most of the loosely bound molecules from the surface resulting in depletion of the amide bands in the IRRAS spectra. The retention of the residual amide band along with the suppression of the bands characteristic of the NHS group is an IR signature of covalent linking between the peptide and the SAM surface. Both TOF-SIMS and IRRAS techniques

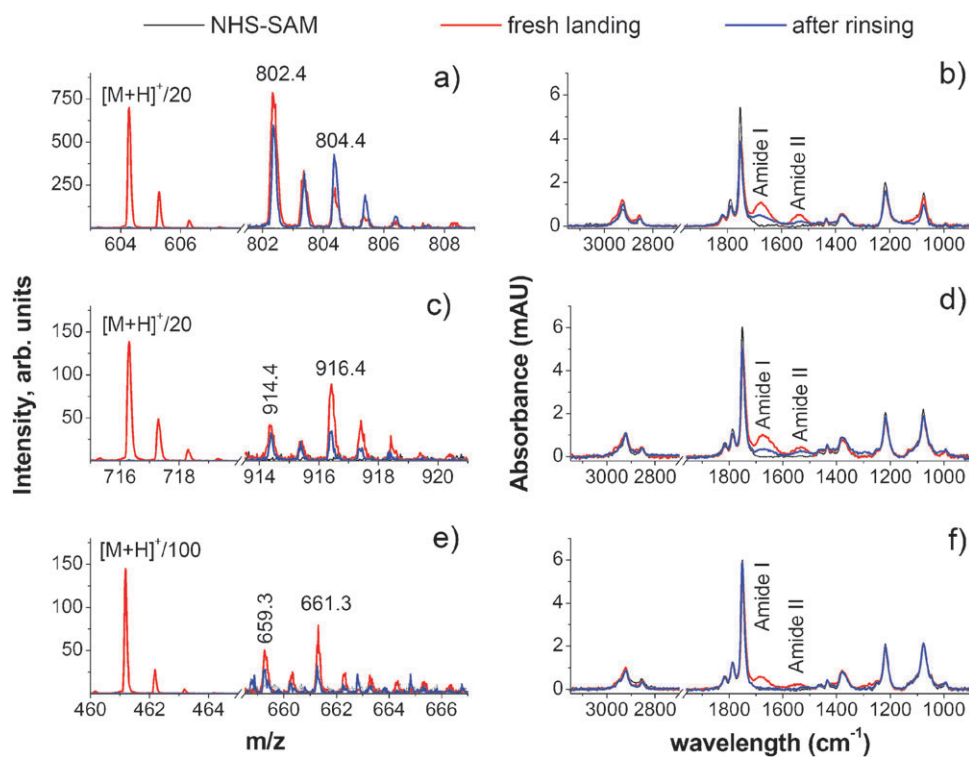


**Fig. 7** ToF-SIMS and IRRAS spectra following soft-landing of  $1.8 \times 10^{13}$  (a) and (b) doubly protonated c-(RGDfK-); (c) and (d) doubly protonated GRGDSPK; (e) and (f) singly protonated RGDGG color code: black: unmodified self-assembled monolayer of N-hydroxysuccinimidyl ester terminated alkylthiol on gold (NHS-SAM); red: NHS-SAM following soft-landing; blue: soft landed sample with extensive rinsing in methanol.

confirm the covalent binding of lysine-containing peptides and indicate very inefficient binding, if any, of the RGDGG peptide that can be linked only through the N-terminal amino group. Interestingly, we found that 4 h reactive landing of GRGDSPK peptide resulted in four times higher local coverage than the local coverage obtained after 15 h of reaction in solution.<sup>41</sup> It follows that reactive landing experiments can promote reactions on surfaces that are characterized by very slow kinetics in solution.

### Factors that affect the efficiency of soft- and reactive landing

The term soft-landing has been used to describe two distinct processes, one in which neutralization occurs during ion-surface collision and one in which the ion preserves its charge. In the earlier discussion we demonstrated that in vacuum the population of both ions and neutral molecules trapped on the surface is depleted by thermal desorption. Loss of the soft-landed material upon exposure of the surface to laboratory air is another important yet poorly quantified factor for experiments that utilize *ex situ* analysis of surfaces. It follows that the efficiency of soft-landing determined experimentally depends both on the efficiency of trapping of the projectile ions or neutral molecules at the time of the collision and on the degree of binding of trapped species to the substrate. The efficiency of reactive landing is a combination of the trapping efficiency and the reactivity of the projectile with the surface. It should be noted that thermal desorption of the linked species

is a very unlikely process because of their strong covalent binding to the substrate.

### Peptide composition and charge state

Deposition of the same number of peptide ions of different size and amino acid composition onto the FSAM surface followed by FT-ICR-SIMS analysis showed that the relative soft-landing efficiencies for different peptides were the same within the experimental uncertainty. The relative values were determined by comparing the total signal of peptide-related peaks observed in FT-ICR SIMS spectra obtained for different projectile ions. In contrast, we found that the efficiency increases with the charge state of the ion. Specifically, the total peptide signal obtained for doubly protonated projectile ions was two times higher than the SIMS signal obtained for the singly protonated precursor.

The efficiency of trapping of ions on surfaces is determined by the attractive potential between the ion and the surface given as a function of the distance,  $D$ , by the following equation:

$$V(R) = -\frac{\alpha(eZ)^2}{2S} \int_0^{\infty} \frac{2\pi r dr}{(\sqrt{r^2 + D^2})^4} = (-) \frac{\pi\alpha(eZ)^2}{2S} \frac{1}{D^2} \quad (4)$$

where  $S$  is the area occupied by the terminal group on the surface,  $e$  is the elementary charge,  $Z$  is the charge state of the ion, and  $\alpha$  is the molecular polarizability of the target. Clearly, the attractive potential between the ion and the surface increases for higher charge states of the projectile ion.

However, eqn (4) predicts quadratic dependence of the trapping efficiency on the charge state of the ion while the experimentally determined relative soft-landing efficiencies showed a linear increase with the charge state of the projectile. It is reasonable to assume that partial neutralization of ions upon collision is responsible for the differences between the trapping efficiency predicted by eqn (4) and the measured soft-landing efficiency.

While the soft-landing efficiency does not show any significant dependence on the peptide composition, reactive landing is strongly affected by the presence and availability of specific functional groups necessary for covalent binding. As mentioned earlier, the efficient formation of amide bond between the peptide and the active ester terminated NHS-SAM surface was observed only for peptides that contain the lysine residue.<sup>41</sup> However, the presence of this residue in the sequence does not necessarily ensure facile covalent linking to the surface. For example, if the structure of the peptide is strongly stabilized by solvation of the lysine residue by backbone carbonyl oxygens of the peptide, the  $\epsilon$ -amino group of the lysine may not be available for reaction during ion-surface collision. It is also interesting that the reaction yield for the c(-RDGfK-) landing onto NHS-SAM surface was independent of the charge state of the precursor ion suggesting that peptide ions undergo efficient neutralization upon collision with this surface.

### Physical and chemical properties of the surface

Physical and chemical properties of the surface determine both the trapping efficiency during collision and the degree of neutralization of the trapped ion on the surface. *In situ* SIMS characterization of several surfaces resulted in very low peptide secondary ion yields following soft-landing on the COOH-SAM surface and much higher yields for the HSAM and FSAM surfaces. In addition, we found that the total peptide-related SIMS signal was *ca.* 2–4 times higher for the FSAM surface as compared to the HSAM. Low sputtered signals obtained for the COOH-SAM were attributed to efficient neutralization of ions on this surface, while the differences between the FSAM and HSAM targets were ascribed to the possible differences in the binding energy between these surfaces and the landed peptides. However, in a follow up TOF-SIMS study we noticed that the total sputtered signal for the unmodified FSAM surface is substantially higher than the total signal obtained for the unmodified HSAM surface suggesting that the relative secondary ion yields obtained for different targets should be normalized to the efficiency of secondary ion formation on these substrates. In addition, little is known about the neutralization efficiencies on the HSAM and FSAM surfaces that have a substantial effect on the observed SIMS signal. While the SIMS analysis is sensitive to the presence of ions on the surface, IRRAS detects the total amount of peptide retained on the surface. Comparable intensities of amide I and amide II bands were observed in IRRAS spectra of Gramicidin S soft-landed on the COOH-SAM and HSAM surfaces<sup>44</sup> suggesting that similar total amounts of neutral and ionic peptide species are retained on these two substrates. Future studies in our laboratory will

address in greater detail the effect of the surface on the efficiency of soft-landing.

The efficiency of reactive landing is a strong function of the barrier for the reaction between the terminal group on the surface and the peptide. It is not surprising that no reaction was observed between lysine-containing peptides and the COOH-SAM surface, while efficient binding was observed for the carboxylic acid terminated SAM activated using the labile NHS ester terminal group.<sup>41</sup> Similar trends were reported for solution-phase reactivity of these substrates. Namely, it has been demonstrated that activation of the COOH-SAM surface with the NHS group expedites the reaction of the monolayer with amine-containing molecules in solution.<sup>72</sup> The reaction efficiency with primary amino groups of the peptides is further improved using carboxylic acid terminated SAMs activated with pentafluorophenyl esters<sup>73</sup> or SAMs terminated with the interchain anhydride.<sup>74</sup>

Physical properties of the SAM surface including the organization of the chains in the monolayer, the density and orientation of the functional groups on the surface, and lateral steric effects also influence the reactivity at the interface. For example, slow reactivity resulting from the confinement effect is expected for well-organized monolayers, while less ordered systems or mixed SAMs, in which reactive terminal groups are more accessible, could substantially improve the yields of reactive landing experiments.

### Collision energy

The kinetic energy of the projectile ion is another important parameter for the soft-landing experiments. It has been demonstrated that at relatively high collision energies collisions of small ions with FSAM and HSAM surfaces result in crash landing, in which the ion undergoes fast fragmentation during the collision and the resulting fragments are retained on the surface.<sup>11</sup>

FT-ICR SIMS analysis of surfaces following soft-landing of peptide ions commonly shows a large number of fragment ions. The extent of fragmentation depends on the composition of the projectile ion and the total abundance of fragment ions ranges from 20 to 80% of the dominant  $[M + H]^+$  signal.<sup>25</sup> Peptide fragmentation observed in SIMS spectra could either result from crash-landing of projectile ions or from internal excitation of the intact peptide on the surface by keV ion desorption during the SIMS analysis. Surprisingly, the same fragmentation pattern was observed in FT-ICR SIMS spectra acquired following soft-landing of doubly protonated bradykinin onto the FSAM surface at several kinetic energies ranging from 0 to 150 eV suggesting that crash-landing does not occur to a significant extent in these experiments and that peptide fragments are generated during the SIMS analysis.<sup>25</sup> It should be noted that TOF-SIMS spectra show very different fragmentation behavior dominated by the formation of characteristic immonium ions and substantially smaller extent of fragmentation.<sup>38</sup> Differences between TOF-SIMS and FT-ICR SIMS spectra are most likely attributed to different timescales of spectral acquisition in these experiments. While TOF-SIMS experiments sample ion population a few microseconds after bombardment, the residence time for ions in

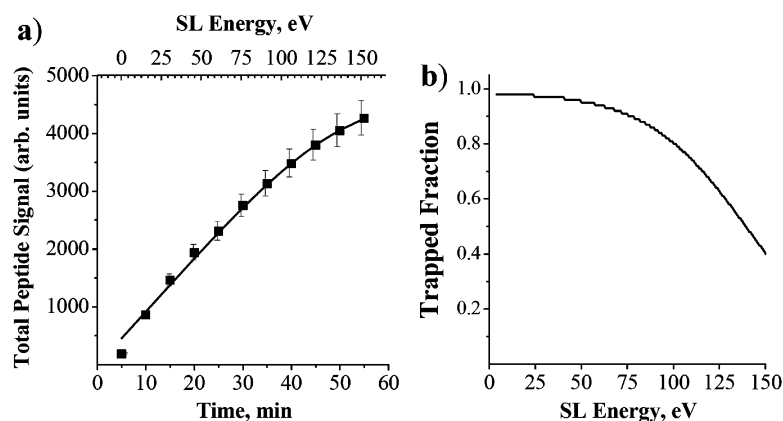


**Fig. 8** (a) Cumulative peptide ion abundance (bradykinin) as a function of time. Top axis shows the corresponding soft-landing energies. The line corresponds to the hard-cube model (see text for details); (b) Trapped fraction as a function of the kinetic energy of soft landed ions calculated using the hard-cube model. Reprinted with permission from Alvarez *et al.*, *J. Phys. Chem. A*, 2006, **110**, 1678. Copyright 2006, American Chemical Society.

FT-ICR SIMS experiments is on the order of 1 s. In a separate experiment we varied the time between the sputtering event and the analysis of the desorbed species in our FT-ICR instrument and found that the extent of fragmentation observed in the FT-ICR SIMS spectra is a strong function of the observation time. These findings further confirm that peptide fragments observed in SIMS spectra are formed in the gas phase from precursor ions excited during the keV bombardment of the surface. The remarkable conclusion obtained from these studies is that soft-landing results in deposition of intact peptide ions onto SAM surfaces even at fairly high collision energies.<sup>25</sup> Similar findings were reported by Turecek and co-workers for soft-landing of crystal violet on plasma-treated silver substrates.<sup>13</sup> Intact deposition of peptides at 150 eV collision energy implies that soft-landed species undergo very fast dissipation of the internal energy deposited into the ion during ion-surface collision.

The dependence of the soft-landing efficiency on the kinetic energy of the projectile ion was studied by exposing the same surface to the ion beam and monitoring the sputtered peptide signal as the kinetic energy was varied.<sup>25</sup> Similar experiment performed using the ion beam of the same collision energy showed a linear increase of the total peptide signal as a function of time. In contrast, when the collision energy is

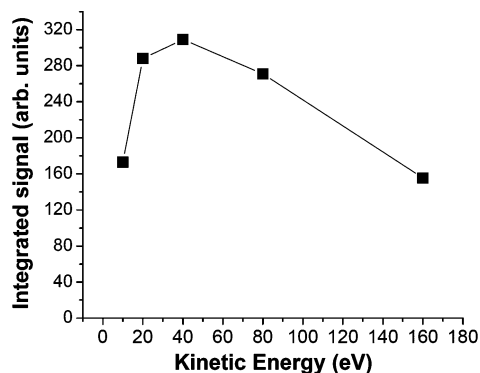


**Fig. 9** Total signal of the covalent adduct integrated over the spot profile as a function of the kinetic energy.

gradually increased from 0 to 150 eV the total peptide signal shows a negative deviation from linearity (Fig. 8a) suggesting that the soft-landing efficiency decreases with increasing collision energy. These results were rationalized using a modified hard-cube model.<sup>75–77</sup> In this model a projectile of mass  $M$  approaches the surface with velocity  $u$  and undergoes an impulsive collision with a hard cube of mass  $m$  moving with a thermal velocity distribution along the surface normal. Grimmelmann *et al.* derived an expression for the fraction of projectiles scattered off such a surface.<sup>77</sup> The trapped fraction obtained using this formalism is shown in Fig. 8b. The slow decrease of the trapped function at low collision energies is followed by a fairly sharp decrease at energies above 100 eV. The decrease in the soft-landing efficiency at high collision energies results from efficient competition between trapping and scattering of projectile ions.

The effect of the initial kinetic energy of the projectile ion on the efficiency of the reactive landing was explored by comparing the reaction yields obtained following deposition of the doubly protonated c(-RGDFK-) onto the NHS-SAM surface over a wide range of collision energies (10–160 eV).<sup>41</sup> Fig. 9 shows the dependence of the reaction efficiency on collision energy. The reaction yield shows a gradual increase at collision energies below 20 eV, followed by a plateau region from 20 to 80 eV, and a decrease at collision energies above 100 eV. The decrease in reaction efficiency observed at high collision energies follows the corresponding decrease in the soft landing efficiency (Fig. 8b) suggesting that at high collision energies the efficiency of reactive landing is determined by the efficiency of ion trapping on the surface. In contrast, at low kinetic energies the reactive landing efficiency is determined by the ability of the system to overcome the reaction barrier resulting in the observed increase in the reaction yield with collision energy.

## Conclusions and future directions

Surface modification by soft-landing of low-energy ions produced using soft ionization techniques provides unique opportunities for selective preparation of a variety of new substrates for applications in biology, biomaterials sciences

and catalysis. Fundamental understanding of soft- and reactive landing is important for designing new applications utilizing these phenomena. In addition, deposition of biomolecules on substrates will assist in obtaining molecular level understanding of interactions of peptides and proteins with hydrophobic and hydrophilic surfaces relevant to transport of biomolecules through membranes in living organisms and determination of binding energies between biomolecules and model surfaces in the absence of solvents.

Reactive landing of mass selected ions provides an opportunity to carry out a variety of interfacial synthetic chemistry experiments. The advantages of this approach include highly selective preparation of the gas-phase reactant and the ability to promote slow reactions by varying the kinetic energy of the projectile ion that results in local heating of the surface upon collision. Many reactive surfaces including metals, semiconductors, polymers and SAMs could be used in reactive landing experiments. SAM surfaces presenting terminal amines, hydroxyls, carboxylic acids, phosphates, aldehydes and halogens are susceptible to different classes of organic reactions, such as nucleophilic substitution, esterification, acylation, nucleophilic addition and other. Different types of molecules including but not limited to peptides, proteins, lipids, oligosaccharides, and dendrimers can be selectively immobilized on surfaces using low-energy ion-surface collisions. In addition, gas-phase ion chemistry can be utilized to generate novel compounds that cannot be readily synthesized in solution for subsequent immobilization by soft-landing.

Our understanding of the factors that determine the efficiency of soft- and reactive landing processes is still very limited. In particular, little is known about the rates and mechanisms of charge reduction and neutralization of large ions on surfaces, the degree of binding of ions and neutral molecules to substrates, the effect of surface composition and morphology on the efficiency of ion deposition and retention. These questions will be addressed in future studies.

## Acknowledgements

This work was supported by the grant from the Chemical Sciences Division, Office of Basic Energy Sciences of the US Department of Energy (DOE), and the Laboratory Directed Research and Development Program at the Pacific Northwest National Laboratory (PNNL). The work was performed at the W. R. Wiley Environmental Molecular Sciences Laboratory (EMSL), a national scientific user facility sponsored by the US DOE of Biological and Environmental Research and located at PNNL. PNNL is operated by Battelle for the US DOE.

## References

- V. Grill, J. Shen, C. Evans and R. G. Cooks, *Rev. Sci. Instrum.*, 2001, **72**, 3149–3179.
- L. Hanley and S. B. Sinnott, *Surf. Sci.*, 2002, **500**, 500–522.
- A. M. Bittner, *Surf. Sci. Rep.*, 2006, **61**, 383–428.
- S. R. Kasi, H. Kang, C. S. Sass and J. W. Rabalais, *Surf. Sci. Rep.*, 1989, **10**, 1–104.
- D. C. Jacobs, *Annu. Rev. Phys. Chem.*, 2002, **53**, 379–407.
- R. G. Cooks, T. Ast and A. Mabud, *Int. J. Mass Spectrom. Ion Processes*, 1990, **100**, 209–265.
- A. R. Dongre, A. Somogyi and V. H. Wysocki, *J. Mass Spectrom.*, 1996, **31**, 339–350.
- B. Gologan, J. R. Green, J. Alvarez, J. Laskin and R. G. Cooks, *Phys. Chem. Chem. Phys.*, 2005, **7**, 1490–1500.
- B. Gologan, J. M. Wiseman and R. G. Cooks, in *Principles of Mass Spectrometry Applied to Biomolecules*, ed. J. Laskin and C. Lifshitz, John Wiley & Sons, Inc., Hoboken, NJ, 2006.
- S. A. Miller, H. Luo, S. J. Pachuta and R. G. Cooks, *Science*, 1997, **275**, 1447.
- J. W. Shen, Y. H. Yim, B. B. Feng, V. Grill, C. Evans and R. G. Cooks, *Int. J. Mass Spectrom.*, 1999, **183**, 423–435.
- H. Luo, S. A. Miller, R. G. Cooks and S. J. Pachuta, *Int. J. Mass Spectrom.*, 1998, **174**, 193–217.
- M. Volny, A. Sengupta, C. B. Wilson, B. D. Swanson, E. J. Davis and F. Turecek, *Anal. Chem.*, 2007, **79**, 4543–4551.
- M. B. J. Wijesundara, L. Hanley, B. R. Ni and S. B. Sinnott, *Proc. Natl. Acad. Sci. U. S. A.*, 2000, **97**, 23–27.
- M. B. J. Wijesundara, E. Fuoco and L. Hanley, *Langmuir*, 2001, **17**, 5721–5726.
- B. Kaiser, T. M. Bernhardt, B. Stegemann, J. Opitz and K. Rademann, *Phys. Rev. Lett.*, 1999, **83**, 2918–2921.
- R. Neuendorf, R. E. Palmer and R. Smith, *Chem. Phys. Lett.*, 2001, **333**, 304–307.
- R. E. Palmer, S. Pratontep and H. G. Boyen, *Nat. Mater.*, 2003, **2**, 443–448.
- M. Mitsui, S. Nagaoka, T. Matsumoto and A. Nakajima, *J. Phys. Chem. B*, 2006, **110**, 2968–2971.
- F. Claeysens, S. Pratontep, C. Xirouchaki and R. E. Palmer, *Nanotechnology*, 2006, **17**, 805–807.
- S. Messerli, S. Schintke, K. Morgenstern, A. Sanchez, U. Heiz and W. D. Schneider, *Surf. Sci.*, 2000, **465**, 331–338.
- W. Yamaguchi, K. Yoshimura, Y. Tai, Y. Maruyama, K. Igarashi, S. Tanemura and J. Murakami, *Chem. Phys. Lett.*, 1999, **311**, 341–345.
- B. Gologan, Z. Takats, J. Alvarez, J. M. Wiseman, N. Talaty, Z. Ouyang and R. G. Cooks, *J. Am. Soc. Mass Spectrom.*, 2004, **15**, 1874–1884.
- J. Alvarez, R. G. Cooks, S. E. Barlow, D. J. Gaspar, J. H. Futrell and J. Laskin, *Anal. Chem.*, 2005, **77**, 3452–3460.
- J. Alvarez, J. H. Futrell and J. Laskin, *J. Phys. Chem. A*, 2006, **110**, 1678–1687.
- M. Volny, W. T. Elam, B. D. Ratner and F. Turecek, *Anal. Chem.*, 2005, **77**, 4846–4853.
- Z. Ouyang, Z. Takats, T. A. Blake, B. Gologan, A. J. Guymon, J. M. Wiseman, J. C. Oliver, V. J. Davisson and R. G. Cooks, *Science*, 2003, **301**, 1351–1354.
- M. Volny, W. T. Elam, A. Branca, B. D. Ratner and F. Turecek, *Anal. Chem.*, 2005, **77**, 4890–4896.
- B. B. Feng, D. S. Wunschel, C. D. Masselon, L. Pasa-Tolic and R. D. Smith, *J. Am. Chem. Soc.*, 1999, **121**, 8961–8962.
- G. Siuzdak, B. Bothner, M. Yeager, C. Brugidou, C. M. Fauquet, K. Hoey and C. M. Chang, *Chem. Biol.*, 1996, **3**, 45–48.
- J. P. Cowin, A. A. Tsekouras, M. J. Iedema, K. Wu and G. B. Ellison, *Nature*, 1999, **398**, 405–407.
- A. A. Tsekouras, M. J. Iedema and J. P. Cowin, *J. Chem. Phys.*, 1999, **111**, 2222–2234.
- S. C. Nanita, Z. Takats and R. G. Cooks, *J. Am. Soc. Mass Spectrom.*, 2004, **15**, 1360–1365.
- L. Gao, M. E. Lyn, D. E. Bergeron and A. W. Castleman, *Int. J. Mass Spectrom.*, 2003, **229**, 11–17.
- D. Loffler, S. S. Jester, P. Weis, A. Bottcher and M. M. Kappes, *J. Chem. Phys.*, 2006, **124**, Art. No. 054705.
- H. J. Rader, A. Rouhanipour, A. M. Talarico, V. Palermo, P. Samori and K. Mullen, *Nat. Mater.*, 2006, **5**, 276–280.
- J. W. Denault, C. Evans, K. J. Koch and R. G. Cooks, *Anal. Chem.*, 2000, **72**, 5798–5803.
- J. Laskin, P. Wang, O. Hadjar, J. H. Futrell, J. Alvarez and R. G. Cooks, *Int. J. Mass Spectrom.*, 2007, **265**, 237–243.
- O. Hadjar, J. H. Futrell and J. Laskin, *J. Phys. Chem. C*, 2007, **111**, 18220–18225.
- P. Wang, O. Hadjar and J. Laskin, *J. Am. Chem. Soc.*, 2007, **129**, 8682–8683.
- P. Wang, O. Hadjar, P. L. Gassman and J. Laskin, submitted to *Phys. Chem. Chem. Phys.*

- 42 J. C. Love, L. A. Estroff, J. K. Kriebel, R. G. Nuzzo and G. M. Whitesides, *Chem. Rev.*, 2005, **105**, 1103–1169.
- 43 U. Reimer, U. Reineke and J. Schneider-Mergener, *Curr. Opin. Biotechnol.*, 2002, **13**, 315–320.
- 44 O. Hadjar, P. Wang, J. H. Futrell, Y. Dessiaterik, Z. Zhu, J. P. Cowin, M. J. Iedema and J. Laskin, *Anal. Chem.*, 2007, **79**, 6566–6574.
- 45 J. Laskin, E. V. Denisov, A. Shukla, S. E. Barlow and J. H. Futrell, *Anal. Chem.*, 2002, **74**, 3255–3261.
- 46 R. G. Cooks, T. Ast, T. Pradeep and V. Wysocki, *Acc. Chem. Res.*, 1994, **27**, 316–323.
- 47 A. Somogyi, T. E. Kane, J. M. Ding and V. H. Wysocki, *J. Am. Chem. Soc.*, 1993, **115**, 5275–5283.
- 48 D. L. Smith, V. H. Wysocki, R. Colorado, O. E. Shmakova, M. Graupe and T. R. Lee, *Langmuir*, 2002, **18**, 3895–3902.
- 49 R. D. Weinstein, J. Moriarty, E. Cushnie, R. Colorado, T. R. Lee, M. Patel, W. R. Alesi and G. K. Jennings, *J. Phys. Chem. B*, 2003, **107**, 11626–11632.
- 50 D. C. Muddiman, A. I. Gusev and D. M. Hercules, *Mass Spectrom. Rev.*, 1995, **14**, 383–429.
- 51 R. Chatterjee, D. E. Riederer, Z. Postawa and N. Winograd, *J. Phys. Chem. B*, 1998, **102**, 4176–4182.
- 52 A. Schnieders, R. Mollers and A. Benninghoven, *Surf. Sci.*, 2001, **471**, 170–184.
- 53 K. H. Park, B. C. Kim and H. Kang, *J. Chem. Phys.*, 1992, **97**, 2742–2749.
- 54 N. Wade, C. Evans, F. Pepi and R. G. Cooks, *J. Phys. Chem. B*, 2000, **104**, 11230–11237.
- 55 N. Wade, C. Evans, S. C. Jo and R. G. Cooks, *J. Mass Spectrom.*, 2002, **37**, 591–602.
- 56 C. Evans, N. Wade, F. Pepi, G. Strossman, T. Schuerlein and R. G. Cooks, *Anal. Chem.*, 2002, **74**, 317–323.
- 57 N. Wade, B. Gologan, A. Vincze, R. G. Cooks, D. M. Sullivan and M. L. Bruening, *Langmuir*, 2002, **18**, 4799–4808.
- 58 T. Pradeep, B. Feng, T. Ast, J. S. Patrick, R. G. Cooks and S. J. Pachuta, *J. Am. Soc. Mass Spectrom.*, 1995, **6**, 187–194.
- 59 S. A. Miller, H. Luo, X. Jiang, H. W. Rohrs and R. G. Cooks, *Int. J. Mass Spectrom. Ion Processes*, 1997, **160**, 83–105.
- 60 J. W. Shen, V. Grill, C. Evans and R. G. Cooks, *J. Mass Spectrom.*, 1999, **34**, 354–363.
- 61 N. Wade, T. Pradeep, J. W. Shen and R. G. Cooks, *Rapid Commun. Mass Spectrom.*, 1999, **13**, 986–993.
- 62 E. T. Ada, O. Kornienko and L. Hanley, *J. Phys. Chem. B*, 1998, **102**, 3959–3966.
- 63 M. B. J. Wijesundara, Y. Ji, B. Ni, S. B. Sinnott and L. Hanley, *J. Appl. Phys.*, 2000, **88**, 5004–5016.
- 64 A. Choukourov, J. Kousal, D. Slavinska, H. Biederman, E. R. Fuoco, S. Tepavcevic, J. Saucedo and L. Hanley, *Vacuum*, 2004, **75**, 195–205.
- 65 G. R. Blacken, M. Volny, T. Vaisar, M. Sadilek and F. Turecek, *Anal. Chem.*, 2007, **79**, 5449–5456.
- 66 D. H. Min and M. Mrksich, *Curr. Opin. Chem. Biol.*, 2004, **8**, 554–558.
- 67 E. Ruoslahti and M. D. Pierschbacher, *Science*, 1987, **238**, 491–497.
- 68 E. Ruoslahti, *Annu. Rev. Cell Devel. Biol.*, 1996, **12**, 697–715.
- 69 U. Hersel, C. Dahmen and H. Kessler, *Biomaterials*, 2003, **24**, 4385–4415.
- 70 J. Lahiri, L. Isaacs, J. Tien and G. M. Whitesides, *Anal. Chem.*, 1999, **71**, 777–790.
- 71 P. Wagner, M. Hegner, P. Kernen, F. Zaugg and G. Semenza, *Biophys. J.*, 1996, **70**, 2052–2066.
- 72 T. P. Sullivan and W. T. S. Huck, *Eur. J. Org. Chem.*, 2003, 17–29.
- 73 A. D. Corbett and J. L. Gleason, *Tetrahedron Lett.*, 2002, **43**, 1369–1372.
- 74 L. Yan, C. Marzolin, A. Terfort and G. M. Whitesides, *Langmuir*, 1997, **13**, 6704–6712.
- 75 R. M. Logan and R. E. Stickney, *J. Chem. Phys.*, 1966, **44**, 195–201.
- 76 R. D. Levine, *Molecular Reaction Dynamics*, Cambridge University Press, Cambridge, UK, 2005.
- 77 E. K. Grimmelmann, J. C. Tully and M. J. Cardillo, *J. Chem. Phys.*, 1980, **72**, 1039–1043.